PETER BACKHAUS[1], BURKHARD SCHMIDT,
AND MARCOS DANTUS[2]

# Control of photoassociation yield: A quantum-dynamical study of the mercury system to explore the role of pulse duration from nanoseconds to femtoseconds [3]

[1]Institut für Physikalische and Theoretische Chemie,
Freie Universität Berlin, Takustraße 3, D-14195 Berlin, Germany
[2]Department of Chemistry and Center for Fundamental Materials Research,
Michigan State University, East Lansing, MI 48824-1322, USA
[3]to appear in: Chemical Physics Letters, 1999

**Abstract**

The photoassociation process shows strong dependence on the temporal duration of the electromagnetic field pulses and their frequencies. This dependence is investigated using quantum mechanical simulations that include all ranges of impact parameters and contributions from bound-to-bound transitions. The photoassociation yield of mercury atoms to produce excimer dimers is enhanced for short (ps) and for ultrashort (fs) pulse durations. Ultrashort laser pulses effectively overlap the entire range of free-to-bound transition, therefore achieving a maximum probability. Short pulses show a maximum in the photoassociation yield when their carrier frequency overlaps a particular free-to-bound spectroscopic resonance. Implications of these calculations on efforts to control bimolecular reactions are discussed.

# 1   Introduction

Photoassociation is one of the least understood photochemical processes.[1,2] This process has recently gained interest because of its role in the generation of ultracold molecules,[3–7] the real time observation of bimolecular reactions,[8,9] and control of bimolecular encounters.[10,11] Here we explore the dependence of the photoassociation cross section on the temporal duration and the carrier frequency of the electromagnetic field that induces it.

Even though most of the work in the area of laser control of chemical reactions has been dedicated to unimolecular processes,[12,13] some groups have begun to investigate how to control bimolecular reactions.[14–17] The yield of a bimolecular reaction is determined by the energy of the collision, relative orientation of the reactants and impact parameter of the encounter. The photoassociation process has been demonstrated to achieve control of these three key parameters.[10,11] Short-pulse photoassociation provides a well-determined initiation time for the reaction as well as an alignment with respect to the laboratory frame. These additional parameters allow very detailed studies of bimolecular chemical reactions. Pulse duration has been shown a useful parameter in the control of unimolecular processes, especially those involving multiphoton processes.[18,19] Here we explore the role of pulse duration on photoassociation yield.

The calculations presented here are based on the photoassociation of mercury atoms to form the diatomic excimer. For this prototypical system experimental results with femtosecond time resolution are available.[8,11] The quantum-mechanical tools for simulation of these experiments, taking into account the incoherent sum of initial scattering states, are also available.[9,10] In this study we use these tools to explore the effects of pulse duration, and hence energetic bandwidth of the pulse due to the transform limit relation between time and energy widths, on the yield of photoassociation. The relevant potential energy curves for this system are shown in
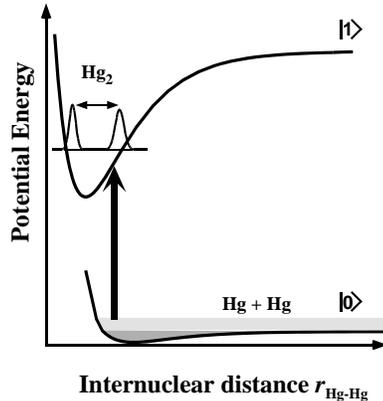
1

Figure 1: Schematic diagram of the photoassociation process. The photon causes a spectroscopic transition from the dissociative (free) continuum states of the electronic ground state to bound levels of the excited electronic state of the excimer system.

Figure 1. A laser pulse with carrier frequency $\omega_p$ causes a free-to-bound transition thus forming a wave packet in the upper state comprising of a coherent superposition of ro-vibrational states. Extension of these results to other similar excimer forming systems, such as Xe + Cl, Kr + F, or Zn + Zn, should be straightforward requiring minor changes in the molecular parameters. For systems involving more atoms these results can be used to provide a quasi-diatomic approximation.

## 2  Model and Methods

The quantum dynamics of photo-induced inelastic scattering of a Hg + Hg collision pair is governed by the time–dependent Hamilton operator

$$\hat{H}(t) = \hat{H}_{\mathrm{mol}} + \hat{W}(t) \quad . \tag{1}$$

In the framework of the Born-Oppenheimer approximation our model of the mercury dimer consists of two electronic states (see Figure 1). In the electronic ground state $X0_g^+$ the two ground state Hg $(6^1S_0)$ atoms are attracted by weak van der Waals forces only. The covalently bound first electronically

excited state $D^3\Sigma_u^+$ is asymptotically connected to mercury atoms in the $(6^1S_0)$ and in the $(6^3P_1)$ states. For simplicity, the two molecular electronic states will be termed $|0\rangle$ and $|1\rangle$. The atomic resonance between these two electronic states corresponds to a wavelength of 253.65 nm.

The time-independent molecular Hamiltonian of the relative motion can be expressed as a function of the internuclear distance vector $\vec{r}$

$$\hat{H}_{\mathrm{mol}}(\vec{r}) = -\frac{\hbar^2}{2m}\frac{1}{r}\frac{\partial^2}{\partial r^2}r + \frac{\hat{J}^2}{2mr^2} + V_{0,1}(r) \tag{2}$$

where $m = 100.99$ u is the reduced mass of $^{202}\mathrm{Hg}_2$ and $\hat{J}$ is the angular momentum of the collision pair. The potential energy curves $V_0(r)$ and $V_1(r)$ of the two electronic states are based on experimental data. We assume Morse potentials with the spectroscopic constants adapted from the literature.[20]

The time-dependent part of the Hamiltonian describes the interaction between the transition dipole moment $\vec{\mu}_{01}$ coupling the two electronic states and an external electric field $\vec{\mathcal{E}}(t)$ in the semi-classical dipole approximation [21]

$$W(t) = -\vec{\mu}_{01}(r) \cdot \vec{\mathcal{E}}(t) = -\mu_{01}(r)\mathcal{E}(t)\cos(\theta) \tag{3}$$

Here it is assumed that $\vec{\mathcal{E}}(t)$ is polarized along the $z$-axis, and $\theta$ is the angle between $\vec{\mu}_{01}$ and $\vec{\mathcal{E}}$. We adapt a transition dipole moment function from the literature using a spline fit to interpolate between the tabulated values.[22] The electric field of the laser pulse can be written as

$$\mathcal{E}(t) = \mathcal{E}_p\, g_p(t)\, \cos(\omega_p t) \tag{4}$$

where $\mathcal{E}_p$ and $\omega_p$ are the amplitude and the carrier frequency of the pulse, respectively. The pulse shape is assumed to be of the form

$$g_p(t) = \sin^2\left(\frac{\pi t}{2T_p}\right), \quad 0 \leq t \leq 2T_p \tag{5}$$

which is similar to a Gaussian function with a full-width at half-maximum (FWHM) of $T_p$ except for the finite wings.

We simulate the quantum dynamics of photo-induced excimer formation of $\mathrm{Hg}_2$ by solving the time-dependent Schrödinger equation in the translational/ vibrational and rotational degrees of freedom using a perturbative treatment detailed by Backhaus et al.[9] which is an extension of earlier work for a rotationless model.[23] Note that the validity of first-order perturbation theory for photoassociation processes has been investigated previously, where an excellent agreement with numerical calculations for field intensities up to $10^{13}$ W/cm$^2$ was shown.[24] This approximation was found to be valid for pulses ranging from one femtosecond to one nanosecond. The photoassociation yield P for a system being initially at energy $E_i$ is then defined

3

as the total population of all the ro-vibrational states of the electronically excited excimer state $|1\rangle$ at the end of the laser pulse $(t = 2T_p)$

$$P(T_p, \omega_p, E_i) := \sum_f |C_f|^2, \tag{6}$$

where the expansion coefficients $C_f$ are obtained as projections of the time–dependent wavepacket onto individual ro-vibrational eigenstates $(f)$ of the excimer state $|1\rangle$

$$C_f \propto \mathcal{E}_p T_p \sum_i S_{fi}\, \mu_{fi}\, G(\Omega_{fi}^\pm, T_p) \tag{7}$$

where $\Omega_{fi}^\pm = \pm\omega_p + (E_f - E_i)/\hbar$ specifies the detuning of the carrier frequency $\omega_p$ with respect to a resonant transition between initial $(i)$ and final $(f)$ states. The summation extends over all initial rotational states the contribution of which is a product of the Hönl-London-Factor $S_{fi}$, the Franck-Condon-factor $\mu_{fi}$, and an effective line-shape function $G$ of the laser pulse. The function G is defined as the Fourier transform of the laser pulse

$$
\begin{aligned}
G(\Omega_{fi}^\pm, T_p) &:= \frac{1}{iT_p} \int_0^{2T_p} dt\, \sin^2\left(\frac{\pi t}{2T_p}\right) \exp\left(i\Omega_{fi}^\pm t\right) \\
&= \frac{\exp\left(i2\Omega_{fi}^\pm T_p\right) - 1}{2\Omega_{fi}^\pm T_p \left[(\Omega_{fi}^\pm T_p/\pi)^2 - 1\right]}
\end{aligned}
\tag{8}
$$

Throughout this work transform-limited pulses will be assumed. Based on the pulse shape defined in Eq. (5), the energetic bandwidth (FWHM) of a pulse is given by

$$\Delta E \times T_p = 4.52\hbar \tag{9}$$

which reads in practical units (eV and fs) as $\Delta E \times T_p \approx 2.975$, e.g. a pulse with a time duration $T_p = 10$ fs has a corresponding energy width, FWHM, $\Delta E \approx 0.3$ eV.

For some of the calculations presented below, a thermal averaging procedure has been applied. The contribution $P_{bb}(T)$ of bound-to-bound transitions to the photoassociation probability is obtained by summing over all ro-vibrational states with the correct statistical (Boltzmann) weights at a specific temperature. For $T = 433$ K the ratio of the concentration of dimers versus monomers is only $f = 3.5 \times 10^{-5}$. The contribution $P_{fb}(T)$ of free-to-bound transitions is calculated as an integral over all different scattering energies weighted with a thermal Maxwell-Boltzmann distribution at $T$ and by summing as many $J$ partial waves as necessary to reach convergence in the photoassociation probability. This was in almost all cases with $J \in [0; 300]$.

# 3   Results

## 3.1   Effect of different pulse lengths

First, we calculate the photoassociation yield $P(T_p, \omega_p, E_i)$ for a free-to-bound transition as a function of the pulse length of the laser and for different carrier frequencies ($\omega_p$). While $T_p$ is varied $\mathcal{E}_p$ is changed such that the energy density per unit area and per laser pulse is kept constant. The initial scattering energy is chosen as $E_i = 27.2$ meV which is close to the maximum of a thermal Maxwell-Boltzmann distribution at $T = 433$ K. Our results are shown in Fig. 2. The association yield features the following two interesting aspects. (1) Starting from 100 fs and shorter pulse lengths, the yield shows a local maximum at approximately 10 fs for each laser frequency. Then it decreases reaching a constant value for the limit of $T_p = 0$ pulse regardless of the frequency because an infinitely short pulse has a white spectrum and the carrier frequency can no longer be defined. (2) For increasing pulse length ($T_p > 100$ fs) the yield exhibits an additional maximum in the region $T_p \in [10^4; 10^6]$ fs for some laser frequencies. These two cases are discussed separately below.
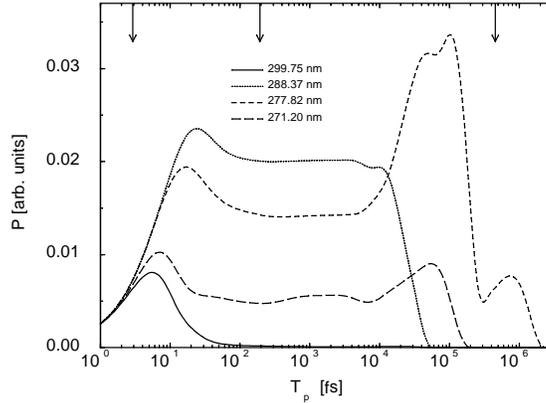


Figure 2: Photoassociation yield $P(T_p, \omega_p, E_i)$ as a function of pulse duration $T_p$ for various frequencies $\omega_p$ and for constant $E_i = 27$ meV. For each curve the total energy density per pulse and unit area was kept constant regardless of pulse duration. The three vertical arrows at the top of the diagram show the characteristic energy of the system in the excimer state $|1\rangle$ which are converted into pulse durations by virtue of Eq. (9), i.e. the well depth ($\approx 1$ eV), the vibrational spacing ($\approx 16$ meV), and the rotational spacing ($\approx 6.6\mu$eV) quantum.

The enhancement of the association-yield in the regime of ultrashort pulses at approximately $T_p \approx 10$ fs can be readily explained by the following

argument. Changing $T_p$ values, the laser pulse changes its energetic distribution. So the number of ro-vibronic states in the $|1\rangle$ state which can be populated in the association process depends on the time $T_p$. In Fig. 3a we plot the $|1\rangle$ ($D_{1u}$) potential for $J = 0$ and the line-shape function $G$ defined in Eq. (8) as a projection on the energy axis for two different $T_p$ values. There are two competing effects that influence the association yield in the ultrashort pulse regime. While for $T_p = 100$ fs the line-shape function encompasses only a limited fraction of the range of bound states of the potential for the excimer state $|1\rangle$, it overlaps almost the entire region for $T_p = 10$ fs resulting in an increase of the association yield. For even shorter pulse lengths, the energetic width exceeds the range of bound states and the association yield decreases again. These competing effects lead to the maximum in the association yield at about 10 fs. This is in qualitative agreement with the time scale of 3 fs obtained from Eq. (9) if we insert the well depth of the excimer state $D_e = 1.0$ eV.
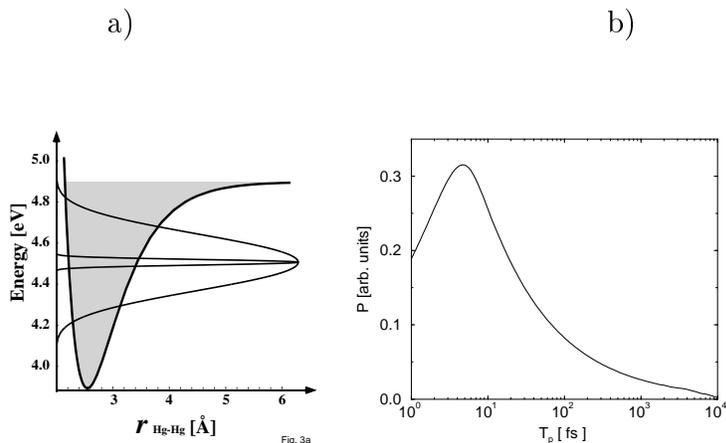
a)                                                                              b)



Figure 3: (a) Limits on pulse duration for enhancing the yield of photoassociation. The $D_{1u}$ state of $Hg_2$ is plotted for $J = 0$ and the line-shape $|G|^2$ of the laser pulse is projected on the energy axis for two different $T_p$ values, 10 fs (broader spectrum) and 100 fs (narrower spectrum). As can be seen for ultrashort pulses there is a complete overlap of the upper state that causes the enhancement for very short pulses. For longer pulses, the enhancement results from spectral resonance to specific ro-vibronic states. (b) Statistical model to calculate the photoassociation probability. This function ignores Franck-Condon and Hönl-London factors. The statistical probability reproduces the enhancement observed at 10 fs for photoassociation shown in Fig. 2.

To further confirm this statistical argument we investigated the overlap

6

between the line-shape of the laser pulse and the density of the ro-vibrational states $\rho(E)$ in the electronically excited state $|1\rangle$ by integrating the product of the density function $\rho(E)$, the line-shape function $G$, and the electric field amplitude $\mathcal{E}_p$. This analysis is equivalent to the full calculation of the association yield, where all Franck Condon and Hönl-London factors are assumed to be equal unity. The electric field amplitude has to be included to keep the pulse energy constant with a varying pulse length $T_p$. The results of this calculation are shown in Fig. 3b. Again we find a maximum near 10 fs similar to the full calculation of the association yield shown in Fig. 2. We conclude that in the ultrafast pulse range of $T_p \leq 10^2$ fs, statistical considerations (overlap of line shape with density of bound states) are sufficient to qualitatively reproduce the behavior of the full calculations.

As can be seen from Fig. 2, the association yield remains constant for the time range $10^2 - 10^4$ fs and eventually falls down to zero for every off-resonance frequency if $T_p$ is chosen long enough. Within our model, which neglects the effect of natural line width due to fluorescence, this is easy to understand in terms of a resonance condition. The association yield is greater than zero only if the energetic window provided by the bandwidth of the laser pulse encompasses at least one ro-vibrational level of the $|1\rangle$ state. This resonance condition depends very sensitively on the carrier frequency $\omega_p$ of the laser pulse. This is demonstrated in Fig. 4 which shows how resonance conditions lead to the enhancements, observed in Fig. 2 for short pulses ($10^4 - 10^5$ fs). In this figure $\omega_p$ is varied in a very small interval between two resonance frequencies. In conclusion, the second maximum in the photoassociation probability depends on resonance with a free-to-bound transition for a certain final ro-vibrational level of the excited state. Furthermore this maximum occurs at pulse durations which are close to those predicted from Eq. (9) if we insert the rotational spacing expected from the $D_{1u} \leftarrow X$ transitions as $\Delta E = 2B = 6.6 \mu$eV, we obtain a pulse duration $T_p \approx 5 \times 10^5$ fs.

## 3.2 Effect of different carrier frequencies

The dependence of the photoassociation yield on the carrier frequency $\omega_p$ of the laser pulse requires particular emphasis on the competing processes of bound-to-bound and free-to-bound transition. We assume a constant pulse duration of $T_p = 100$ fs and a temperature of 433 K. In Fig. 5 the resulting contributions $P_{bb}$ and $P_{fb}$ to the association yield are shown as a function of wavelength.

The initial bound states are all within a relatively narrow energy regime of 46 meV corresponding to the shallow potential well of the electronic ground state. For $\lambda < 290$ nm ($\omega_p > 4.3$ eV) there is a sharp threshold for the onset of bound-to-bound transitions where the photon energy is sufficient to reach the lowest ro-vibrational levels of the excimer. Further
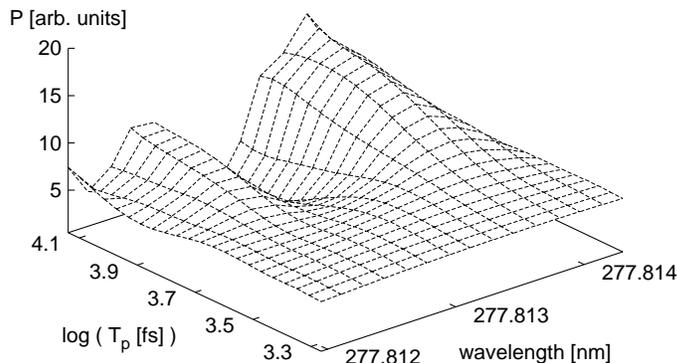
Figure 4: Photoassociation with long pulses. Photoassociation with long laser pulses depends strongly on spectral resonance. Here the probability of photoassociation is plotted as a function of pulse duration and wavelength. Notice that the resonance condition is relaxed as the pulse duration decreases.

increase of $\omega_p$ (decrease of $\lambda$) reduces $P_{bb}$ because the Franck-Condon factors for excitation into higher excimer levels are decreasing as the Franck-Condon window moves towards larger internuclear distances. Around $\lambda = 260$ nm ($\omega_p \approx 4.8eV$) the signal approaches zero since no bound states are available for shorter wavelengths (absorption due to free atoms is not taken into account here). Competition between $P_{fb}$ and $P_{bb}$ in the (260 nm $< \lambda <$ 290 nm) range is governed by the monomers vs. dimers ratio in the sample.

The differences between $P_{fb}$ and $P_{bb}$ arise from the fact that for free-to-bound transitions the scattering energy adds to the photon energy. This additional energy leads to a small spectral shift ($\approx 2-3$ nm) towards longer wavelengths. In addition, the spectral intensity exhibits a long tail towards longer wavelengths (290 nm $< \lambda <$ 335 nm) due to free-to-bound transitions from scattering states above the dissociation energy of the ground state, whose Franck-Condon factors decrease slowly with increasing scattering energy. Therefore, in this range bound-to-bound transitions are not energetically accessible and the signal can be entirely attributed to photoassociation.[8-11]

The simulated data can be compared with experimentally obtained photoassociation spectra. One such example is the work by Jones et al. where the photoassociation spectra of Kr + F and that of Xe + I were compared.[25] Those experiments were carried out with a high spectral reso-
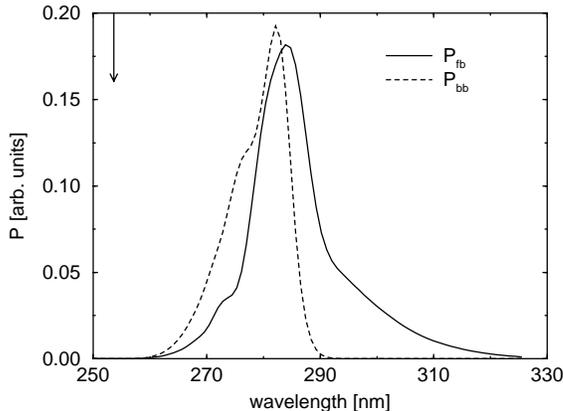
8

Figure 5: Thermally averaged photoassociation yields for $T = 433$ K. The contributions from bound-to-bound $P_{bb}$ and free-to-bound $P_{fb}$ transitions to the total yield are shown individually. The pulse duration for this calculation is $T_p = 100$ fs, and it has a broad enough spectrum that no discrete transitions can be identified. The vertical arrow indicates the atomic transition $(6^3P_1 \leftarrow 6^1S_0)$ at 253.65 nm. Free atomic absorption and radiative lifetime broadening have been ignored for these calculations.

lution (0.2 cm$^{-1}$) laser. The results clearly show resonance enhancement due to excitation of free to bound ro-vibrational states. These resonances are washed out when short and ultrashort pulses are used.

# 4    Discussion and Conclusions

The results of our study show photoassociation yield enhancements for the regime of ultrashort and short pulse durations. These effects cannot be understood from simple arguments based on the rate of hard-sphere collisions. Quantum mechanical calculations show interplay between the density of states available for spectroscopic transitions and spectroscopic resonance. We assume that the observed enhancements will have an impact in the choice of lasers for particular photoassociation experiments. The laser pulse duration, and hence its energetic bandwidth, must match the characteristic energy scales of the system. Enhancements depend on overlapping the entire excited state potential or at least several ro-vibronic states of the product molecule (see the vertical arrows at the top of Fig. 2). These time scales qualitatively indicate the regime of pulse lengths where enhancement of the association yield is expected and thus allow an easy transferability to other

9

diatomic systems. The availability of intense sources of ultrashort laser pulses will permit exploration of a wide range of photoassociation processes.

One of the exciting applications for the photoassociation process is to achieve control of bimolecular reactions. As has been demonstrated in the present work, the wavelength can be used to exclude the possibility of van der Waals precursor complexes and, hence, to select only true bimolecular collision events. Moreover, the photoassociation wavelength has been shown to control the range of impact parameters and overall energy of the collision complex.[10,11] Calculations on the O + H $\rightarrow$ OH and H + Cl $\rightarrow$ HCl system have shown that for systems with large vibrational and/or rotational quanta photoassociation can be used to selectively populate single ro-vibrational states of the product.[24,26,27] The study presented here spans the whole range of pulse durations and hence bandwidths. Implications of our findings apply to studies using ultrafast lasers, where molecular dynamics are time-resolved, to studies using narrow bandwidth lasers, where individual spectroscopic transitions are resolved.

## Acknowledgements

## References

1. S. Mrozowski, Z. Physik 106(1937) 458.

2. V.S. Dubov, L.I. Gudzenko, L.V. Gurvich and S.I. Iakovlenko, Chem. Phys. Lett. 45 (1977) 330.

3. P.D. Lett, P.S. Julienne, and W.D. Phillips, Annu. Rev. Phys. Chem. 46 (1995) 423.

4. S.D. Gensemer and P.L. Gould, Phys. Rev. Lett. 80 (1998) 936.

5. A. Fioretti, D. Coomparat, A. Crubellier, O. Dulieu, F. Masnou-Seeuws and P. Pillet, Phys. Rev. Lett. 80 (1998) 4402.

6. H. Wang, and W.C. Stwalley, J. Chem. Phys. 108 (1998) 5767.

7. A. Vardi, D. Abrashkevich, E. Frishman and M. Shapiro, J. Chem. Phys. 107 (1997) 6166.

8. U. Marvet and M. Dantus, Chem. Phys. Lett. 245 (1995) 393.

9. P. Backhaus and B. Schmidt, Chem. Phys. 217 (1997) 131.

10. P. Gross and M. Dantus, J. Chem. Phys. 106 (1997) 8013.

11. U. Marvet, Q. Zhang and M. Dantus, J. Phys. Chem. A 102 (1998) 4111.

12. Chemical Reactions and their Control on the Femtosecond Time Scale. XXth Solvay Conference on Chemistry, P. Gaspard, and I. Burghardt (Eds.), Adv. Chem. Phys. 101 (1997).

13. R. J. Gordon and S.A. Rice, Annu. Rev. Phys. Chem. 48 (1997) 601.

14. J. L. Krause, M. Shapiro and P. Brumer, J. Chem. Phys. 92 (1990) 1126.

15. P. Brumer and M. Shapiro, Adv. Chem. Phys. 101 (1997) 295.

16. E.D. Potter, J.L. Herek, S. Pedersen, Q. Liu and A.H. Zewail, Nature 355 (1992) 66.

17. V.A. Apkarian, J. Chem. Phys. 106 (1997) 5298.

18. M. Machholm, and A. Suzor-Weiner, J. Chem. Phys. 105, 971 (1996)

19. A. Assion, T. Baumert, J. Helbing, V. Seyfried and G. Gerber, Chem. Phys. Letters 259, 488 (1996)

20. J. Koperski, J.B. Atkinson, and L.Krause, Chem. Phys. Lett. 219 (1994) 161.

21. R. Loudon, The quantum theory of light. Clarendon, Oxford (1973).

22. E.W. Smith, R.E. Drullinger, M.M. Hessel, and J. Cooper, J. Chem. Phys. 66 (1997) 5667.

23. M. Machholm, A. Giusti-Suzor, and F.H. Mies, Phys. Rev. A 50 (1994) 5025.

24. P. Backhaus, J. Manz, and B. Schmidt, J. Phys. Chem. A 102 (1998) 4118.

25. R. B. Jones, J. H. Schloss and J. G. Eden, J. Chem. Phys. 98 (1993) 4317.

26. M.V. Korolkov and B. Schmidt, Chem. Phys. 272 (1997) 96.

27. M.V. Korolkov and B. Schmidt, Chem. Phys. Lett. 237 (1998) 123.